

Phenomenological simulation and density functional theory prediction of ^{57}Fe Mössbauer parameters: application to magnetically coupled diiron proteins

Jorge H. Rodriguez

Published online: 29 January 2013
© Springer Science+Business Media Dordrecht 2013

Abstract The use of phenomenological spin Hamiltonians and of spin density functional theory for the analysis and interpretation of Mössbauer spectra of antiferromagnetic or ferromagnetic diiron centers is briefly discussed. The spectroscopic parameters of the hydroxylase component of methane monooxygenase (MMOH), an enzyme that catalyzes the conversion of methane to methanol, have been studied. In its reduced diferrous state (MMOH_{Red}) the enzyme displays ^{57}Fe Mössbauer and EPR parameters characteristic of two ferromagnetically coupled high spin ferrous ions. However, Mössbauer spectra recorded for MMOH_{Red} from two different bacteria, *Methylococcus capsulatus* (Bath) and *Methylosinus trichosporium* OB3b, display slightly different electric quadrupole splittings (ΔE_Q) in apparent contradiction to their essentially identical active site crystallographic structures and biochemical functions. Herein, the Mössbauer spectral parameters of MMOH_{Red} have been predicted and studied via spin density functional theory. The somewhat different ΔE_Q recorded for the two bacteria have been traced to the relative position of an essentially unbound water molecule within their diiron active sites. It is shown that the presence or absence of the unbound water molecule mainly affects the electric field gradient at only one iron ion of the binuclear active sites.

Keywords DFT · Spin hamiltonian · ^{57}Fe Mössbauer · Density functional theory · Uteroferrin · Purple acid phosphatase · Methane monooxygenase

Electronic supplementary material The online version of this article (doi:10.1007/s10751-012-0744-y) contains supplementary material, which is available to authorized users.

Supported, in part, by NSF CAREER Award CHE-0349189 (JHR).

J. H. Rodriguez (✉)
Department of Physics, Purdue University, West Lafayette, IN 47907, USA
e-mail: jhrodrig@purdue.edu

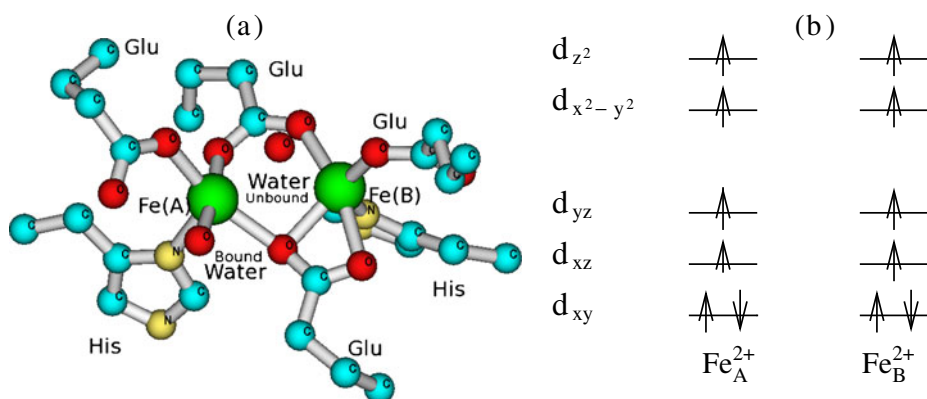


Fig. 1 **a** Optimized geometric structure of the diferrous site of methane monooxygenase hydroxylase in its reduced state (MMOH_{Red}). Coordinates used for optimization taken from a reported crystallographic structure. [8] **b** Ferromagnetic configuration of valence electron shell of Fe_{A,B}²⁺ ions in MMOH_{Red}

1 Introduction

Binuclear iron (i.e. diiron) proteins and related model compounds often exhibit highly informative but fairly complex ⁵⁷Fe Mössbauer spectra [1, 2]. Mössbauer data recorded as a function of temperature and applied magnetic field can provide a significant amount of information provided that it is properly analyzed. The complexity of spectra of diiron motifs is due, in part, to interactions between valence electrons *fairly* localized on different iron ions. In diiron proteins some of the most relevant intermetallic interactions are not direct but indirect. That is, valence electrons of different iron ions often interact with each other *via* atomic or molecular orbitals of their common bridging ligands. O²⁻ and OH⁻, for example, not only act as *structural bridges* between two irons in some proteins but their valence orbitals also act as *electronic bridges* which allow 3d shells of different metals to interact with each other [3]. Such bridge mediated interactions, e.g. Fe³⁺-O²⁻-Fe³⁺ and Fe³⁺-OH⁻-Fe³⁺, are called collectively *superexchange* and can lead to antiferromagnetic or ferromagnetic coupling [3–5]. The binuclear center of the enzyme methane monooxygenase hydroxylase in its reduced (diferrous) state (MMOH_{Red}), in particular, is ferromagnetic as illustrated by Fig. 1 [6, 7].

The individual ions forming diiron cores in proteins, herein labeled Fe_A^{X+} and Fe_B^{X+}, can be in a number of oxidation states (i.e. X = 2, 3, or 4) and are often found in high spin states (e.g. S_{A,B} = $\frac{4}{2}$ or $\frac{5}{2}$) represented by spin angular momentum operators **S**_A and **S**_B, respectively. In terms of theoretical analysis and interpretation of Mössbauer spectra of spin coupled diiron centers, however, the most relevant spin operators are not necessarily those corresponding to individual iron ions. Instead, the total spin operator **S** = **S**_A + **S**_B may be used to represent the binuclear system in an alternative or complementary fashion. That is, from the perspective of certain experiments, the net anti- or ferro-magnetic coupling between the metal ions leads

the entire binuclear core to behave as a single, magnetically ordered, unit which may be described in terms of a single spin operator, namely that representing the total spin (\mathbf{S}) or of its eigenvalues $S_A + S_B$, $S_A + S_B - 1$, ..., $S_A - S_B$. The intermetallic interactions responsible for magnetic ordering can be collectively represented by the Heisenberg-Dirac-Van Vleck Hamiltonian

$$\mathcal{H}_{HB} = J_{HB} \mathbf{S}_A \cdot \mathbf{S}_B \quad (1)$$

where the operator $\mathbf{S}_A \cdot \mathbf{S}_B$ has the same eigenstates as \mathbf{S} since the commutation condition applies, namely $[\mathbf{S}_A \cdot \mathbf{S}_B, \mathbf{S}] = 0$. In the notation of (1) positive and negative values of J_{HB} correspond to antiferromagnetic and ferromagnetic ordering, respectively. The strength of the coupling between the metal ions is given by the Heisenberg exchange constant (J_{HB}) which, for oxo- or hydroxo-bridged complexes, can take dramatically different values as determined from fits to susceptibility data [9, 10]. In addition, relatively recent advances in the phenomenological simulation of spectra have allowed determination of J_{HB} from fits of low temperature Mössbauer spectra recorded in applied magnetic fields [1, 11]. Likewise, very accurate values for J_{HB} [3, 12] as well as isomer shifts, quadrupole splittings [13], and zero-field splittings [14, 15] have been predicted, in an *ab-initio* based computational approach, from spin unrestricted density functional theory (SDFT). Herein, we briefly summarize the phenomenological approach for the simulation of spectra of spin coupled binuclear iron centers as well as the SDFT-based methodology to accurately predict Mössbauer parameters. In addition, as an application of the methods described in here, we present results that shed light on the physico-chemical origin of the Mössbauer spectral parameters corresponding to the ferromagnetic state of the diiron-containing enzyme methane monooxygenase.

2 Theoretical and computational methods

From an *ab initio* perspective, spectral features can be related to two defining and closely related characteristics of the diiron centers, namely (i) many body effects [11, 16] such as intra- and inter-atomic valence electron interactions, and (ii) molecular structure. Accurately predicting Mössbauer parameters from an *ab initio* perspective, however, has been a difficult task and some advances in this field will be discussed in the next subsection. For historical and practical reasons, however, it is convenient to initially describe a phenomenological (i.e. non *ab initio*) and yet remarkably informative methodology, namely spectral fitting based on spin Hamiltonians and the use of genetic searching algorithms.

2.1 Phenomenological simulation of applied field spectra

Simulation based on spin Hamiltonians can be used to extract a vast amount of information from Mössbauer spectra of diiron centers recorded in applied magnetic fields. In this approach one represents the relevant interactions in terms of *intrinsic*,

as opposed to *fictitious*, electron ($\mathbf{S}_{i=A,B}$) and nuclear ($\mathbf{I}_{i=A,B}$) spin operators. This provides a fairly fundamental way to relate recorded spectra to physico-chemical parameters. Herein, we describe a spin Hamiltonian appropriate for the interpretation and simulation of Mössbauer spectra of spin-coupled diiron centers [1, 2, 11]:

$$\mathcal{H} = JS_A \cdot \mathbf{S}_B + \sum_{i=A}^B \{ \mathbf{S}_i \cdot \tilde{D}_i \cdot \mathbf{S}_i + \beta \mathbf{S}_i \cdot \tilde{g}_i \cdot \mathbf{H} + \mathbf{S}_i \cdot \tilde{a}_i \cdot \mathbf{I}_i + \mathbf{I}_i \cdot \tilde{P}_i \cdot \mathbf{I}_i - \beta_n g_n \mathbf{H} \cdot \mathbf{I}_i \} \quad (2)$$

where \mathcal{H} includes isotropic Heisenberg exchange, zero-field splitting, electronic Zeeman, magnetic hyperfine, electric quadrupole, and nuclear Zeeman interactions, respectively. The first three terms of (2), corresponding to electronic interactions, can also be used to simulate data from other techniques such as electron paramagnetic resonance (EPR) and magnetic susceptibility [4] and can be grouped as an electronic Hamiltonian ($\mathcal{H}_{\text{elec}}$). The last three terms of (2) include interactions with the nuclear environment and can be grouped as a nuclear Hamiltonian ($\mathcal{H}_{\text{nuclear}}$). Accordingly, (2) can be visualized as the combination of two components

$$\mathcal{H} = \mathcal{H}_{\text{elec}} + \mathcal{H}_{\text{nuclear}} \quad (3)$$

In the case of diiron centers, $i = A, B$ correspond to Fe_A and Fe_B , respectively. Importantly, explicit inclusion of individual ion interactions within the summation in (2) allow for simultaneous simulation of spectra of binuclear centers composed of, often, chemically non-equivalent iron ions. For example, the individual and fairly different spectral contributions from the Fe^{3+} ($S_A = 5/2$) and Fe^{2+} ($S_B = 4/2$) ions of the antiferromagnetic protein uteroferrin have been clearly elucidated by application of (2) [1] as shown in Fig. 2.

The well defined, but fairly large, number of interactions required to fit spectra based on (2) makes the task of finding an optimal set of spin Hamiltonian parameters highly nontrivial. In the absence of an efficient computational procedure the problem appeared hopeless as stated by Frauenfelder in 1972 “The complexity of this Hamiltonian requires a computer program for a meaningful solution. If all tensors are allowed to have different principal axes systems, 27 parameters are to be determined for the two-iron unit” [17]. Even more parameters need to be fitted if iron impurity species are present in the sample in addition to the protein diiron center. In 1996 Rodriguez, Debrunner et al. [1, 2] published a major computational advance towards determining an optimal set of spin Hamiltonian parameters, namely *via* application of *genetic* searching algorithms. The success of this searching methodology for parametrization of (2) has been illustrated by their analysis of applied field spectra of the diiron proteins uteroferrin [1] and hemerythrin [11] as well as binuclear model compounds [2]. In addition, the same formalism allows diagonalization of the electronic component of (3) and computation of g -values which can be directly compared with those measured by EPR [18]. Such combined fit of Mössbauer and EPR data ensures that a single set of spin Hamiltonian parameters is found which is consistent with both experimental techniques (Fig. 2).

Despite their great usefulness, one main limitation of simulations based on spin Hamiltonians is the difficulty in establishing a direct and clear relationship between fitted physico-chemical parameters and geometric structure. By contrast, accurate *ab initio*-based predictions of Mössbauer parameters have become possible in recent years and, by necessity, rely on and are sensitive to subtle structural features and geometric variations of the iron-containing complexes.

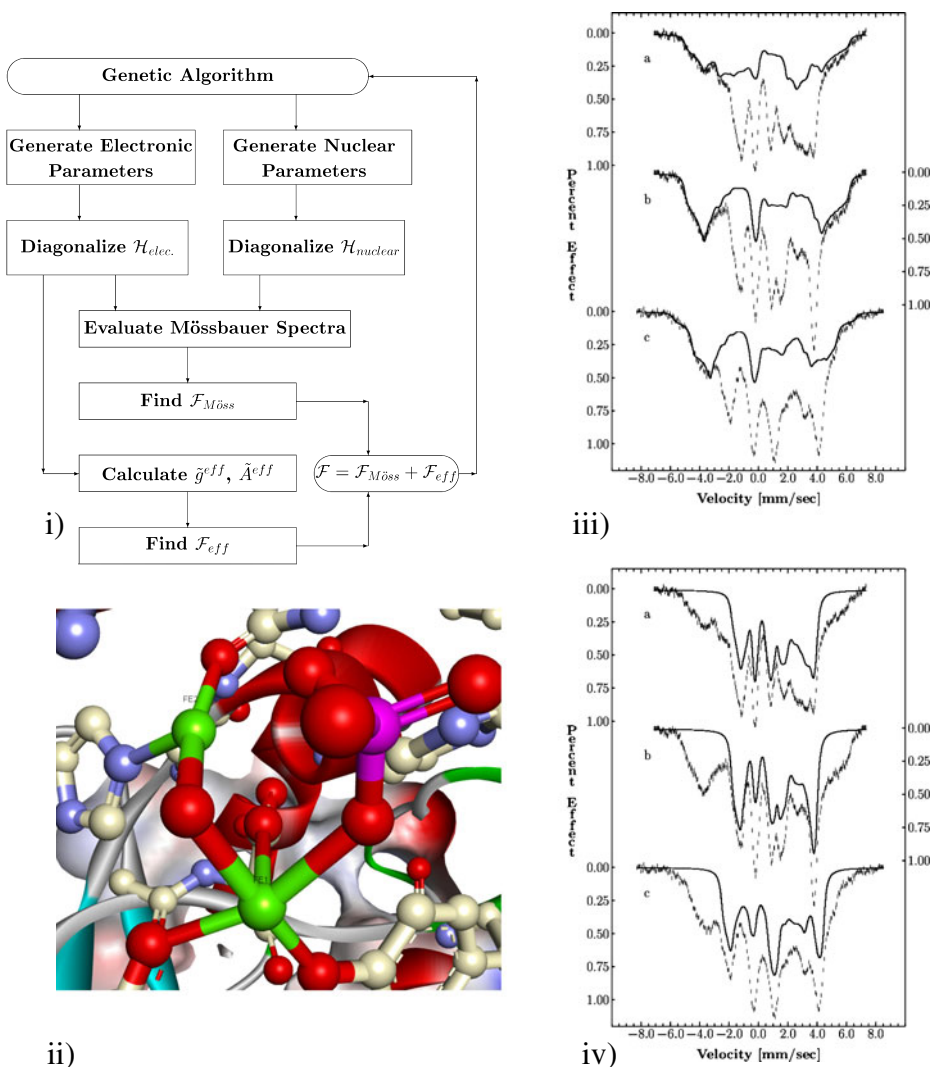


Fig. 2 **i** Diagram representing search procedure for finding an optimal set of spin Hamiltonian parameters. Values of parameters associated with electronic and nuclear Hamiltonians defined in (3) are generated by a *genetic* algorithm to simultaneously fit Mössbauer spectra and EPR g values [1]. **ii** Crystallographic structure of the phosphate bound diiron center of uteroferrin. Iron and oxygen atoms shown in green and red, respectively. **iii–iv** Individual contributions from Fe^{3+} (S=5/2) and Fe^{2+} (S=2) sites of reduced uteroferrin to 4.2 K Mössbauer spectra recorded under (a) 0.032 T (*perpendicular*), (b) 0.032 T (*parallel*), and (c) 3.7 T (*parallel*) applied fields. Figures reproduced from Rodriguez et al. [1] *Solid lines* generated from (2)

2.2 Prediction of ^{57}Fe Mössbauer parameters *via* SDFT

Spin unrestricted density functional theory (SDFT) allows an *ab-initio* treatment of iron-containing molecular and biomolecular complexes by computing the total $\rho(\mathbf{r}) = \rho^\alpha(\mathbf{r}) + \rho^\beta(\mathbf{r})$ and spin $\rho^s(\mathbf{r}) = \rho^\alpha(\mathbf{r}) - \rho^\beta(\mathbf{r})$ electron densities. This requires

explicit numerical solution of two sets of *pseudo* eigenvalue Kohn-Sham equations corresponding to spin up (α) and spin down (β) electrons [19–21]:

$$\left[-\frac{1}{2}\nabla^2 + v_{eff}^{\alpha,\beta}(\mathbf{r}) \right] \phi_i^{\alpha,\beta}(\mathbf{r}) = \epsilon_i^{\alpha,\beta} \phi_i^{\alpha,\beta}(\mathbf{r}) \quad (4)$$

In (4), $\phi_i^{\alpha,\beta}(\mathbf{r})$ are the Kohn-Sham molecular orbitals hosting spin up or down electrons, respectively. The effective potential $v_{eff}^{\alpha,\beta}(\mathbf{r})$ includes, in addition to the potential generated by the nuclei, the classical and non-classical electron-electron interactions *via* the *functional derivatives* of the Coulomb potential energy $\delta J[\rho(\mathbf{r})]/\delta\rho(\mathbf{r})$ and of the exchange-correlation energy $\delta E_{xc}[\rho^\alpha(\mathbf{r}), \rho^\beta(\mathbf{r})]/\delta\rho^{\alpha,\beta}(\mathbf{r})$, respectively.

SDFT [19–21] allows the calculation of the electron density and other properties of spin-polarized (ferromagnetic or antiferromagnetic) systems. In the case of antiferromagnetic states corresponding to open-shell singlets (for which the spin density $\rho^s(\mathbf{r})$ does not vanish everywhere), one can compute a spin-polarized electron density [3, 22] which formally *resembles* that of a true open shell singlet. Once a Kohn-Sham single Slater determinant has been obtained from SDFT calculations, one can compute the electron density at the nucleus of a particular iron ion, i.e. $\rho_i(\mathbf{r} = 0)$ ($i = A, B$), and also the corresponding electric field gradient (EFG) tensor in its principal axes $\tilde{V}_i = (V_{xx,i}, V_{yy,i}, V_{zz,i})$. In a second stage, $\rho_i(\mathbf{r} = 0)$ and \tilde{V}_i which have been determined from SDFT calculations, can be used to determine their interaction with monopole and quadrupole moments of ^{57}Fe nuclei thus predicting δ_{Fe} and ΔE_{Q} , respectively [13, 23]. To implement this latter stage, different groups have used their own, often relatively similar, approaches [23–27]. Chachiyo and Rodriguez [13] recently reported a particularly accurate procedure for the computation of δ_{Fe} and ΔE_{Q} based on the following expressions:

$$\delta_{\text{Fe}} = c_a^{\text{IS}} \rho_i(\mathbf{r} = 0) + c_b^{\text{IS}} \quad (5)$$

$$\Delta E_{\text{Q}} = c^{\text{QS}} V_{zz,i} (1 + \eta^2/3)^{\frac{1}{2}} \quad (6)$$

where ρ_i and $V_{zz,i}$ are computed with an all electron basis (6-311G*, 5D, 7F) [28, 29] and the B3LYP [30] exchange-correlation functional. The constants $c_a^{\text{IS}} = -0.32767921$ mm/s and $c_b^{\text{IS}} = +3806.7754$ mm/s, being functional and basis set dependent, are the slope and intercept for a linear fit of computed $\rho_i(\mathbf{r} = 0)$ versus experimental δ_{Fe} for a training set of iron complexes. Similarly, $c^{\text{QS}} = -1.42129$ mm/s was obtained from a fit of computed V_{zz} versus experimental ΔE_{Q} .

3 Results and discussion

3.1 Mössbauer spectral parameters of diferrous MMOH

The electronic structure and spectroscopic parameters of the hydroxylase component of soluble methane monooxygenase (MMOH), an enzyme that catalyzes the conversion of methane to methanol, have been studied. In its reduced diferrous state (MMOH_{Red}) the enzyme displays ^{57}Fe Mössbauer and EPR parameters characteristic of two ferromagnetically coupled high spin ferrous ions (Table 1) [6, 31]. However, Mössbauer spectra recorded for MMOH_{Red} from two different bacteria, *Methylococcus capsulatus* (Bath) and *Methylosinus trichosporium* OB3b, display

Table 1 Experimental Mössbauer spectral parameters for iron sites of MMOH_{Red} in *Methylococcus capsulatus* (Bath) and *Methylosinus trichosporium* OB3b

Ref.	T [K]	Γ [mm/s]	Fe _A		Fe _B	
			$\delta_{\text{Fe}}^{\text{Exp}}$ [mm/s]	$\Delta E_{\text{Q}}^{\text{Exp}}$ [mm/s]	$\delta_{\text{Fe}}^{\text{Exp}}$ [mm/s]	$\Delta E_{\text{Q}}^{\text{Exp}}$ [mm/s]
<i>M. capsulatus</i> (Bath)						
[7]	80		+1.30	(na)3.01	+1.30	(na)3.01
[32]	4.2	≈0.8	+1.30	(na)2.87	+1.30	(na)2.87
<i>M. trichosporium</i> OB3b						
[31]	153		+1.26	(na)3.07	≈+1.3	≈(na)1.9
[31]	103		+1.26	(na)3.12	≈+1.3	≈(na)2.1
[31]	4.2		+1.30	(na)3.14	≈+1.3	≈(na)2.4
[6]	4.2		≈+1.30	≈ +3.1	≈+1.3	≈ +2.4–3.0

slightly different electric quadrupole splittings (ΔE_{Q}) in apparent contradiction to their essentially identical active site crystallographic structures and biochemical functions. Herein, the Mössbauer spectral parameters of MMOH_{Red} have been predicted and studied based on SDFT calculations.

The experimental isomer shifts and quadrupole splittings for the diiron centers of *M. capsulatus* (Bath) and *M. trichosporium* OB3b display similarities but also subtle differences. As shown in Table 1, *M. capsulatus* (Bath) displays, at 4.2 K in zero field, one broad quadrupole doublet ($\Gamma \approx 0.8$ mm/s) consistent with some inequivalence of the iron sites and/or inhomogeneity of the protein environment [32]. The isomer shifts for two independent measurements, at 80 K and 4.2 K, are essentially identical (+1.30 mm/s). The corresponding quadrupole splittings are, however, somewhat different (3.01 and 2.87 mm/s) as shown in Table 1. Whereas some temperature dependence is expected for ΔE_{Q} of ferrous sites, a change of ≈ 0.14 mm/s may also reflect minor differences in the coordination environment of the iron sites from measurement to measurement. This may be due to positional fluctuations of the nominally unbound water molecule illustrated in Fig 1. Such a slight change in coordination environment becomes even more likely as one analyzes the reported temperature dependence for ΔE_{Q} of Fe_A in *M. trichosporium* OB3b. Namely, as the sample temperature changes from 153 K to 4.2 K, ΔE_{Q} for Fe_A increases by ≈ 0.07 mm/s (Table 1). By contrast ΔE_{Q} of Fe_A in *M. capsulatus* (Bath) decreases by a greater amount over a smaller temperature range.

M. trichosporium OB3b displays greater coordination inequivalence of the two ferrous sites as reflected in their measured quadrupole splittings. Whereas for two independent sets of measurements the isomer shifts of both iron sites are, at the same temperature of 4.2 K, close to +1.3 mm/s, the corresponding quadrupole splittings differ from site to site. Fe_A yields $\Delta E_{\text{Q}} \approx 3.1$ mm/s whereas Fe_B displays a range of values, $\Delta E_{\text{Q}} \approx 2.4$ –3.0 mm/s, which are centered at 2.7 mm/s [6]. Therefore, the experimental parameters suggest that the electric field gradient at Fe_A is fairly constant due to i) a fairly unique coordination environment regardless of the sample used in the measurements or ii) dominance of certain chemical bonds which are not subject to fluctuations such as those associated with a loosely bound water molecule. By contrast, the broad range of ΔE_{Q} values produced by Fe_B at the same temperature (i.e. 4.2 K) indicate substantial differences in its electric field gradient from measurement to measurement and/or diiron center inhomogeneities within the same sample due to lack of compliance with of one or both of the above

Table 2 Predicted Mössbauer parameters for iron sites of MMOH_{Red}

Unbound H ₂ O	Iron site	Mössbauer parameters				
		$\rho_i(0)$ [a_0^{-3}]	$\delta_{Fe}^{Computed}$ [mm/s]	V_{zz} [a.u.]	η	$\Delta E_Q^{Computed}$ [mm/s]
Yes	Fe _A	11613.976	+1.12	-2.203420	0.27290	+3.17
	Fe _B	11614.133	+1.07	-2.010795	0.07603	+2.86
No	Fe _A	11614.113	+1.07	-2.071446	0.49612	+3.06
	Fe _B	11614.214	+1.04	-1.834209	0.20584	+2.63

mentioned conditions. To elucidate the physico-chemical origin of the broad range of experimental quadrupole splittings associated with Fe_B, for the same temperature and/or the same sample, we carried out geometry optimizations (Tables S1 and S2) and SDFT-based calculations to predict ΔE_Q both in the presence and absence of the nominally unbound water. Table 2 shows how the absence of the water introduces a relatively minor change (0.11 mm/s) in the ΔE_Q of Fe_A but a greater change in that of Fe_B (0.23 mm/s). Thus, the SDFT calculations show that the relative position, or even absence, of the unbound water within the diiron active site of MMOH_{Red} mainly affects the EFG of only one iron site (i.e. Fe_B) consistent with the experimental ΔE_Q values shown in Table 1. We postulate that the range of values observed for Fe_B is likely due to the greater sensitivity of the EFG at this site to positional variations of the unbound water molecule. Future MD calculations may confirm this hypothesis. Finally, computed δ_{Fe} are lower, by ≈ 0.18 – 0.26 mm/s, than experimental values. This suggests that the coordination of the iron ions in the crystallographic structure (used as the starting point for the predictions) and in solution (used for the measurements) are not identical. In solution, each iron may be coordinated to a water [33].

References

- Rodriguez, J.H., Ok, H.N., Xia, Y.M., Debrunner, P.G., Hinrichs, B.E., Meyer, T., Packard N.: J. Phys. Chem. **100**, 6849 (1996)
- Rodriguez, J.H., Xia, Y.M., Debrunner, P.G., Chaudhuri, P., Wieghardt, K.: J. Am. Chem. Soc. **118**, 7542 (1996)
- Rodriguez, J.H., McCusker, J.K.: J. Chem. Phys. **116**, 6253 (2002)
- Bencini, A., Gatteschi, D.: EPR of Exchange Coupled Systems. Springer Verlag, Berlin (1990)
- Kahn, O.: Molecular Magnetism. VCH, New York (1993)
- Fox, B.G., Hendrich, M.P., Surerus, K.K., Andersson, K.K., Froland, W.A., Lipscomb, J.D., Münck, E.: J. Am. Chem. Soc. **115**, 3688 (1993)
- DeWitt, J.G., Bentsen, J.G., Rosenzweig, A.C., Hedman, B., Green, J., Pilkington, S., Papaefthymiou, G.C., Dalton, H., Hodgson, K.O., Lippard, S.J.: J. Am. Chem. Soc. **113**, 9219 (1991)
- Whittington, D.A., Lippard, S.J.: J. Am. Chem. Soc. **123**, 827 (2001)
- Armstrong, W.H., Lippard, S.J.: J. Am. Chem. Soc. **105**, 4837 (1983)
- Armstrong, W.H., Lippard, S.J.: J. Am. Chem. Soc. **106**, 4632 (1984)
- Rodriguez, J.H., Xia, Y.M., Debrunner, P.G.: J. Am. Chem. Soc. **121**, 7846 (1999)
- Rodriguez, J.H.: In: Matta, C.F. (ed.) Quantum Biochemistry, pp. 537–549. Wiley-VCH Verlag GmbH & Co. KGaA (2010)
- Chachiyo, T., Rodriguez, J.H.: Dalton Trans. **41**, 995 (2012)
- Aquino, F., Rodriguez, J.: J. Chem. Phys. **123**, 204902 (2005)
- Aquino, F., Rodriguez, J.H.: J. Phys. Chem. A **113**, 9150 (2009)
- McWeeny R.: J. Chem. Phys. **42**, 1717 (1965)
- Frauenfelder, H., Gunsalus, I.C., Münck, E.: In: Mössbauer Spectroscopy and its Applications, pp. 231–255. IAEA, Vienna (1972)

18. Sage, J.T., Xia, Y.M., Debrunner, P.G., Keough, D.T., De Jersey, J., Zerner, B.: *J. Am. Chem. Soc.* **111**, 7239 (1989)
19. Kohn, W., Sham, L.J.: *Phys. Rev.* **140**, A1133 (1965)
20. Kohn, W., Becke, A.D., Parr, R.G.: *J. Phys. Chem.* **100**, 12974 (1996)
21. Parr, R.G., Yang, W.: *Density-functional Theory of Atoms and Molecules*. Oxford University Press, New York (1989)
22. Noodleman, L.: *J. Chem. Phys.* **74**, 5737 (1981)
23. Oldfield, E.: *Philos. Trans. R. Soc. Lond. Ser. B* **360**, 1347 (2005)
24. Yamada, Y., Tominaga, T.: *J. Radioanal. Nucl. Chem. Letters* **188**, 83 (1994)
25. Havlin, R.H., Godbout, N., Salzmann, R., Wojdelski, M., Arnold, W., Schulz, C.E., Oldfield, E.: *J. Am. Chem. Soc.* **120**, 3144 (1998)
26. Bochevarov, A.D., Friesner, R.A., Lippard, S.J.: *J. Chem. Theory Comput.* **6**, 3735 (2010)
27. Han, W.-G., Noodleman, L.: *Inorg. Chem.* **47**, 2975 (2008)
28. Hehre, W.J., Radom, L., Schleyer, P.v.R., Pople, J.A.: *Ab Initio Molecular Orbital Theory*. John Wiley & Sons, New York (1986)
29. Frisch, M.J., et al.: *Gaussian 09, Revision A.1*. Gaussian, Inc., Wallingford, CT (2009)
30. Becke, A.D.: *J. Chem. Phys.* **98**, 5648 (1993)
31. Fox, B.G., Surerus, K.K., Münck, E., Lipscomb, J.D.: *J. Biol. Chem.* **263**, 10553 (1988)
32. Liu, K.E., Valentine, A.M., Wang, D.L., Huynh, B.H., Edmondson, D.E., Salifoglou, A., Lippard, S.J.: *J. Am. Chem. Soc.* **117**, 10174 (1995)
33. The author thanks a manuscript reviewer for suggesting this possibility